

Room temperature coherent spin-alignment of silicon vacancies in 4H- and 6H-SiC

Victor A. Soltamov, Alexandra A. Soltamova, and Pavel G. Baranov*
Ioffe Physical-Technical Institute, St. Petersburg, 194021 Russia

Ivan I. Proskuryakov
Institute of Basic Biological Problems RAS, Pushchino 142290, Russia
 (Dated: February 28, 2012)

Optically induced inverse population of the ground state spin sublevels of the silicon vacancies in silicon carbide (SiC) at room temperature was observed for the first time, making them a very favorable defect for spintronics and quantum information processing. Room temperature transient nutations of the silicon vacancy spin in SiC after optical flash clearly demonstrate that the probed silicon vacancy spin ensemble can be prepared in a coherent superposition of the spin states. Very long coherence times of $\gtrsim 80 \mu\text{s}$ were obtained at room temperature in our experiments even in crystals with high concentrations of the silicon vacancies. Two opposite schemes of the optical alignment of the populations between the ground state spin sublevels of the silicon vacancy are revealed in 4H- and 6H-SiC at room temperature upon illumination with unpolarized light.

PACS numbers: 61.72.Hh, 71.55.-i, 76.70.Hb, 61.72.jd

Detection and manipulation of the spin states in solids at room temperature is a basis of the emerging fields of quantum information processing and spintronics. The first system on which such manipulations were realized at room temperature was the nitrogen-vacancy (NV) center in diamond. Owing to its unique optical excitation cycle that leads to the optical alignment of triplet sublevels of the defect ground state, single NV center can be easily initialized, manipulated and readout by means of optically detected magnetic resonance (ODMR)¹⁻⁴. A search for systems possessing unique quantum properties of the NV defect in diamond that can extend the functionality of such systems seems to be a very promising objective.

On the basis of theoretical predictions and experimental data several other centers were proposed as the candidates comparable with the NV center in diamond. Among them such centers as nitrogen-vacancy center^{5,6}, silicon-carbon divacancy^{7,8} and silicon vacancy (V_{Si})^{9,10} in silicon carbide were proposed. Recently it was experimentally shown that several defect spin states in 4H-SiC can be optically addressed and coherently control at temperatures from 20 to 300 K⁸.

Silicon carbide is a wide-band-gap semiconductor with a well developed growth and doping technology that opens wide possibilities for scalable applications. The isotopic engineering of SiC crystals can be performed through the sublimation crystal growth¹¹, which allows to reduce the natural abundance of ^{29}Si (4.7%) and ^{13}C (1.1%) nuclear spins. SiC can be crystallized in many different polytypes that arise from differences in the stacking sequence of the Si and C layers. The most common polytypes are 4H- and 6H-SiC. In 4H-SiC two nonequivalent crystallographic positions exist, one hexagonal and one quasicubic called h and k , respectively. In 6H-SiC three nonequivalent positions are formed, one hexagonal (h) and two quasicubic ones (k_1 and k_2) (see Fig. 1(a) and 3(a)). Due to the difference in the surrounding envi-

ronments, a defect located at the h and k site often has different properties.

Vacancies are the primary defects in SiC incorporated at various sites in different polytypes. Both photoluminescence (PL) and electron paramagnetic resonance (EPR) spectra of these centers vary depending on their position in the crystal lattice. Unusual polarization properties of various vacancy defects in SiC were observed by means of EPR under optical excitation and reported for the first time in the work of Vainer and Il'in¹². Observation of the low temperature optical spin alignment of the V_{Si} ground state and zero-field ODMR studies at 1.4 K were reported in Ref. [10]. Here we show that two opposite schemes for the optical alignment of the spin sublevels in the ground state of a silicon vacancies in 4H- and 6H-SiC can be realized even at room temperatures and that spin ensemble can be prepared in a coherent superposition of the spin states.

Crystals of two main SiC polytypes were studied in the present work: 4H-SiC and 6H-SiC. Silicon vacancies were introduced by irradiation with fast neutrons at room temperature with a dose of 10^{15} cm^{-2} - 10^{16} cm^{-2} . The samples, in the shape of platelets, had dimensions of about $3 \times 4 \times 0.4 \text{ mm}^3$ and were oriented for rotation in the $\{11\bar{2}0\}$ plane. The concentration of vacancies under the study in both samples is $\sim 10^{15} \text{ cm}^{-3}$. The precise concentrations are not required for the following analysis.

Flash-induced continuous wave (cw) direct-detection EPR (DD-EPR) technique was used¹³ at the X-band. The EPR signal obtained after the microwave mixer was amplified by wide-band amplifiers and sampled by a boxcar integrator (SR 250, Stanford Research Systems) triggered by the flashes. The sample was excited with 6 ns flashes (ca. 1.5 mJ per flash) from a parametric oscillator LP603 pumped by a Nd-YAG laser LQ 529B (Solar Laser Systems, Byelorussia), which was operated at a repetition rate of 11 Hz and 0.8 nm FWHM. The high-time resolution (ca. 50 ns) allowed signal detection shortly after the

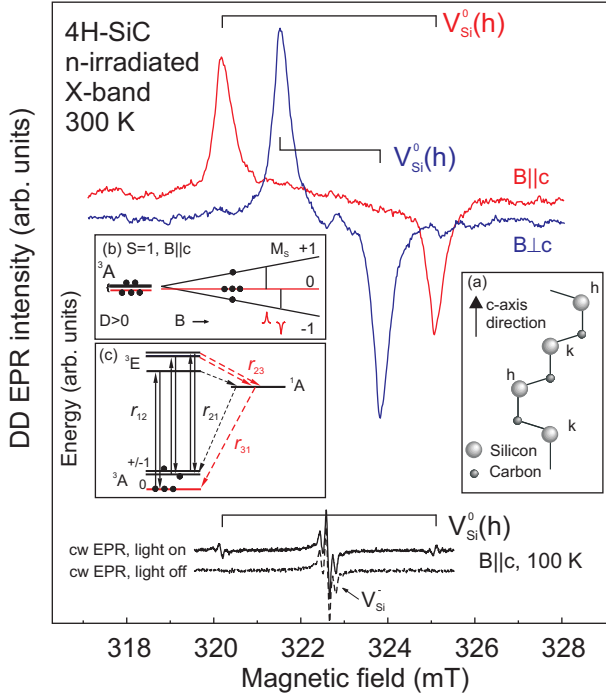


FIG. 1. Flash-induced cw DD-EPR spectra recorded at room temperature in the 4H-SiC crystal under excitation at the wavelength of 890 nm for $B||c$ and $B\perp c$ orientations; (bottom) cw X-band EPR spectra detected under continuous optical illumination and in dark with $B||c$ at $T = 100$ K; (a) Structure of the 4H-SiC polytype; (b) Zeeman levels diagram for the V_{Si}^0 ground state ($S=1$) with the $M_S = 0$ sublevel predominantly populated due to the optical alignment; (c) Seven-level model interpreting the optical alignment of the ground-state sublevels in zero magnetic field.

excitation laser flash, before any significant relaxation between spin sublevels had taken place. To increase a signal/noise ratio, up to 50 field scans were averaged. In the DD-experiment the signal appeared in direct absorption and emission mode.

Conventional cw X-band EPR spectra of the silicon vacancies detected under continuous optical illumination and in dark for $B||c$ orientation at 100 K is shown in Fig. 1 (bottom). The central signal, marked by arrow is attributed to the negatively charged Si vacancy with $S = 3/2$, and zero-field splitting parameter D close to zero¹⁴. This signal is optically silent and discussed somewhere else¹⁶. Lines with the zero-field splitting parameter of $22 \times 10^{-4} \text{ cm}^{-1}$ (65.9 MHz) labeled as V_{Si}^0 are observed under optical illumination and belong to the silicon vacancy. To date the spin state of the V_{Si} giving rise to this splitting is under debate. While we support the model of the neutral V_{Si}^0 with $S=1$, in Ref. [15] it was suggested that such type of EPR spectra belong to the low-symmetry modification of the well-studied negatively charged Si vacancy in the regular environment with $S=3/2$. In our opinion, the authors have not presented sufficiently convincing arguments in favor of the

revision of the model. We will further concern that these signals belong to the neutral V_{Si}^0 with $S=1$. The lines are accompanied by the pair of the hyperfine (HF) lines with a splitting of 0.29 mT due to the HF interaction with twelve equivalent Si atoms of the second shell of the Si vacancy. As expected, under optical pumping at 100 K, the intensity of the EPR spectra grew substantially and a phase reversal was observed for one of the two transitions¹⁰.

Flash-induced cw DD-EPR signals of the V_{Si}^0 recorded at room temperature in the 4H-SiC crystal for two orientations of magnetic field: parallel ($B||c$) and perpendicular ($B\perp c$) to the c axis are shown in the upper part of the Fig.1. The sample was selectively excited into the absorption band of the V_{Si}^0 at 890 nm. The same type of the EPR signal was also observed with the excitation light at wavelengths of 865, 900 and 917 nm. Vertical bars indicate the positions of the lines for the V_{Si}^0 vacancy in the h site for the parallel and perpendicular orientations.

Observed DD-EPR spectra can be described with standard spin Hamiltonian

$$\hat{H} = g\mu_B B \hat{S}_z + D(\hat{S}_z^2 + 1/3S(S+1)) \quad (1)$$

where μ_B is the Bohr magneton, g - is the isotropic g -factor ($g=2.0032$), $S=1$. For 4H-SiC the zero-field splitting parameter D of the V_{Si}^0 was found to be $22 \times 10^{-4} \text{ cm}^{-1}$ (65.9 MHz) for the h site¹⁶.

For the high field transitions the emission instead of absorption is detected, thus we can conclude that optical excitation at room temperature results in establishment of the inverse population between certain sublevels, i.e. optical alignment of the ground spin sublevels. Zeeman levels diagram for the V_{Si}^0 ground state is shown in Fig. 1(b). The populations of the ground state energy sublevels under optical pumping are indicated by different numbers of filled circles. The emission observed for the high-field component of the EPR spectra is due to predominant population of the $M_S=0$ sublevel.

To explain the photokinetic process leading to the spin alignment under optical pumping, we adopt the seven-level model proposed in Ref.¹⁷ for the NV centers in diamond and adopted in Ref.¹⁰ to explain observed DD-EPR spectra of V_{Si}^0 under optical pumping, which suggests the existence of the non-radiative recombination channel. Level diagram shown in Fig. 1(c) comprises 3A ground state, 3E excited state for which only three lower sublevels are depicted, and one singlet 1A state. Optical transition between the 3A and 3E states is spin conserving (solid lines in Fig. 1(c)). In addition, triplet-singlet intersystem crossing (ISC) due to the spin-orbit coupling between 3E and 1A levels occurs. The centers in the $M_S=\pm 1$ sublevels have significantly higher probability to undergo the ISC, thus, the rate r_{23} of the non-radiative transition from the $M_S=\pm 1$ sublevels of the excited 3E state to the metastable singlet 1A state is much larger than the rates of the transition from the $M_S=0$ sublevel. Subsequent decay from the 1A to the $M_S=0$ sublevel of the 3A ground state also occurs with

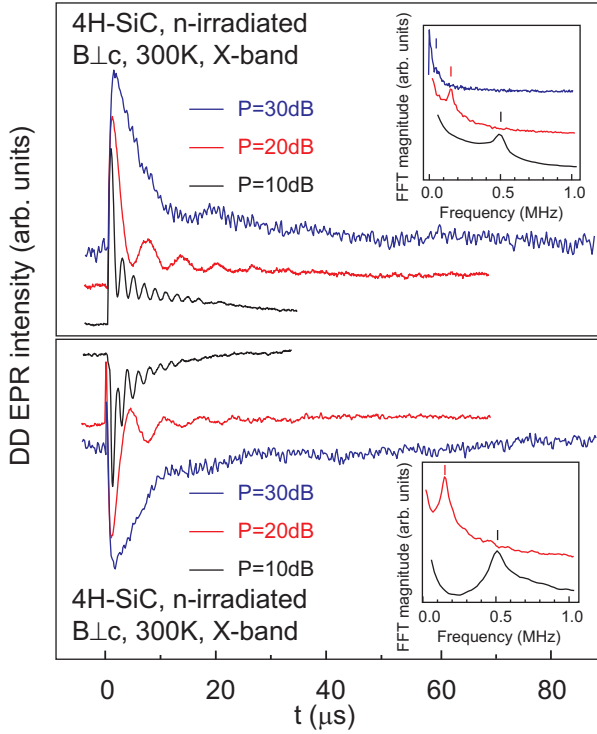


FIG. 2. Transient nutations for the V_{Si}^0 center in 4H-SiC at room temperature are shown for three values of microwave power: the positive traces stand for absorption ($B_0=321.5$ mT), and the negative traces - for emission ($B_0=323.8$ mT) of microwaves. Absolute mw power value is estimated as ca. 5 mW at 10 dB attenuation; (inserts) Corresponding Fourier transform.

the higher rate (r_{31}) than that between 1A and $M_S=\pm 1$. As a result the $M_S=0$ sublevel becomes predominantly populated. As the $M_S=0$ sublevel has a higher probability of fluorescence due to the non-radiative nature of the ISC, the fluorescence intensity between 3E and 3A is spin-dependent. The discussed scheme is true for the V_{Si} center in the h -site of the 4H-SiC lattice at room temperature and is similar to the NV defects in diamond. This type of polarization results in a giant decrease of the photoluminescence intensity observed in the ODMR experiments in zero magnetic field¹⁰.

In Fig. 2, the transient nutations for the V_{Si}^0 center in 4H-SiC at room temperature are shown for three values of microwave power P at $B_0=321.5$ mT (top) and $B_0=323.8$ mT (bottom). In the experiment, the microwave absorption intensity resonant with the spin transitions for two EPR lines (Fig. 1, $B \perp c$) is monitored as a function of the time duration (t) after optical flash. The transition nutation decays due to inhomogeneity of B_1 microwave field over the sample. In addition, the resonance frequencies are also spread around some mean value of resonance Larmor frequency $\langle \omega_0 \rangle$ leading to the inhomogeneous line-broadening.

Clearly, the observed oscillatory behavior demonstrates that the probed V_{Si}^0 spin ensemble can be prepared

in a coherent superposition of the spin states at resonant magnetic fields at room temperatures. The population difference of spin states becomes modulated in time with the Rabi frequency given by $\omega_1 = \gamma_e B_1$, where γ_e is the gyromagnetic ratio for electron. The Fourier transforms corresponding to observed oscillations are presented in the inserts of Fig. 2. The Rabi frequencies are $\omega_1=0.02$ MHz, 0.16 MHz, and 0.5 MHz at $P=30$ dB, 20 dB and 10 dB. Rabi oscillations decay with a characteristic time constant τ_R that depends on the microwave power (Fig. 2). Empirically, τ_R is generally smaller than the coherence time¹⁸ (T_2), thus the lower limit of T_2 is determined to be of about 80 μs at room temperature.

Transient nutation experiment allows to establish the fact that the coherence can be created. From this experiment the pulse duration for the application of a $\pi/2$ -pulse and a π -pulse can be established. It follows that the length of a $\pi/2$ -pulse is approximately 1 μs for microwave power of 10 dB and 4.2 μs , respectively, for 20 dB. This information will be of crucial importance for electron spin echo and ODMR experiments at room and above room temperatures.

Figure 3 shows the flash-induced cw DD-EPR signals in the 6H-SiC crystal detected at room temperature and 100 K in $B \perp c$ orientation of magnetic field. The sample is selectively excited into the absorption band of the V_{Si}^0 . Vertical bars indicate the positions of the lines of the V_{Si}^0 vacancy in the hexagonal h and two quasi-cubic sites ($k1, k2$). Conventional cw X-band EPR spectra of the Si vacancies detected under continuous optical illumination and in dark with $B \perp c$ at 100 K is shown at the bottom for comparison. The spectra are described with standard spin Hamiltonian (eq. (1)) with $D = 42.8 \times 10^{-4} \text{ cm}^{-1}$ (128.3 MHz) and $9 \times 10^{-4} \text{ cm}^{-1}$ (26.9 MHz) for h and k sites of 6H-SiC, respectively¹⁶.

As can be seen from Fig. 3 another type of the optical alignment is realized for the V_{Si}^0 in the h -site in the 6H-SiC at room temperature^{9,10}. To explain the emissive nature of the low-field transition, Zeeman levels diagram for the V_{Si} ground state is shown in the inset (Fig. 3). The population differences between sublevels are indicated by the different numbers of circles. Such population differences induced by the optical pumping can be explained if we suggest the existence of spin-dependent non-radiative decay path via 1E level in the optical cycle. The decay rate r_{23} from the $M_S=\pm 1$ sublevels of the excited 3E state to the metastable 1E state¹⁷ is again much larger than the rates of transition from the $M_S=0$ sublevel, but, on contrast to the V_{Si} in 4H-SiC, the rates of the transitions r_{31} between the 1E state and $M_S=0$ sublevel of the ground state are much smaller than the rates of the transitions from the 1E to the $M_S=\pm 1$ sublevels of the ground 3A state. Thus, the spin sublevels with $M_S=\pm 1$ of the 3A ground state are predominantly populated. This type of polarization results in a giant increase of the photoluminescence intensity observed in the ODMR experiments in zero magnetic field^{9,10}.

As was noted the spin state of the silicon vacancy is

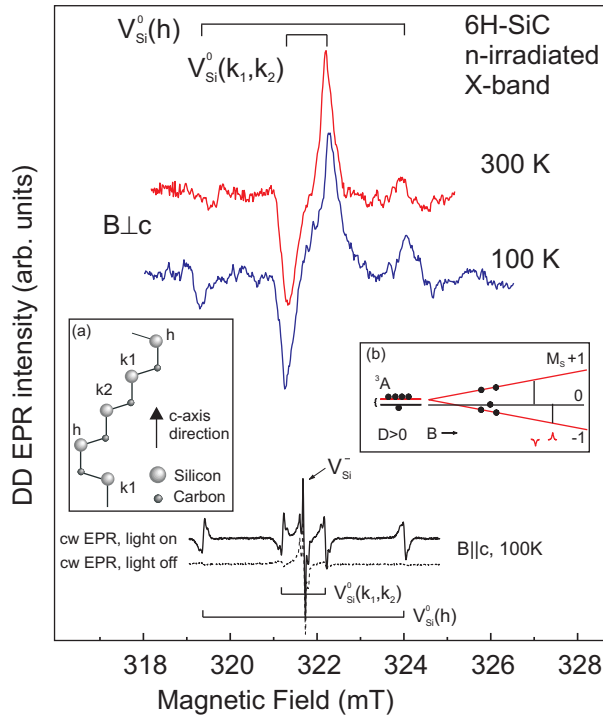


FIG. 3. Flash-induced cw DD-EPR spectra recorded at room temperature and 100 K in the 6H-SiC crystal under excitation at 890 nm for $B \perp c$ orientation; (bottom) Conventional cw X-band EPR spectra detected under continuous optical illumination and in dark with $B \perp c$ at 100 K; (a) Structure of the 6H-SiC polytype; (b) Zeeman levels diagram for the V_{Si}^0 ground state ($S=1$); $M_S = \pm 1$ sublevels predominantly populated due to the optical alignment.

still under debate. However, there is no doubt that the high-spin state is the ground state of the silicon vacancy thus the similar alignment processes can be valid for the

$S=3/2$ system. In principle the mechanism of spin alignment should remain almost the same with the only difference that the $M_S=\pm 1$ and $M_S=0$ sublevels should be replaced by $M_S=\pm 3/2$ and $M_S=\pm 1/2$, respectively. For this model $M_S=\pm 1/2$ sublevels should be equally populated and the existence of a metastable doublet state instead of singlet state should be assumed.

To conclude, optically induced inverse population of the ground state spin sublevels of the simplest intrinsic defect that can be designed in the nuclear magnetic moment free surrounding, Si vacancy in 4H- and 6H-SiC, was observed for the first time at room temperature. In distinction from the known NV defect in diamond¹, and recently observed defects in SiC⁸, two opposite schemes for the optical alignment of the populations of the spin sublevels in the ground state of V_{Si}^0 in 4H- and 6H-SiC were observed at room temperature upon illumination with unpolarized light. Based on the measured transient nutations of the EPR signal intensity estimated coherence time is expected to be longer than 80 μs at room temperature. Zero-field splitting parameters for V_{Si}^0 in 4H- and 6H-SiC are much lower than that of the NV center in diamond ($D=2.87$ GHz for NV center) and recently observed defects in SiC. Thus the V_{Si}^0 can be manipulated by the low-energy radiowave quanta in the range of 20-150 MHz, depending on the position of the silicon vacancy in the crystal lattice, which is one-two orders of magnitude lower than the energy required to manipulate the NV defect in diamond and neutral carbon-silicon divacancy in SiC.

This work has been supported by Ministry of Education and Science, Russia, under the Contracts No. 14.740.11.0048 and 16.513.12.3007; the Programs of the Russian Academy of Sciences: "Spin phenomena in solid state nanostructures and spintronics"; "Fundamentals of nanostructure and nanomaterial technologies" and by the Russian Foundation for Basic Research.

* Pavel.Baranov@mail.ioffe.ru

- ¹ A. Gruber, A. Drabenstedt, C. Tietz, et al., Science **276**, 2012 (1997).
- ² F. Jelezko, J. Wrachtrup, Phys. Stat. Sol. (a) **203**, 3207 (2006).
- ³ F. Jelezko, I. Popa, A. Gruber, et al., Appl. Phys. Lett. **81**, 2160 (2002).
- ⁴ A. P. Nizovtsev, S. Ya. Kilin, F. Jelezko, et al., Physica B **340-342**, 106 (2003).
- ⁵ J. R. Weber, W. F. Koehl, J. B. Varley, et al., PNAS, **107**, 8513 (2010).
- ⁶ D. DiVincenzo, Nature Materials **9**, 468 (2010).
- ⁷ P. G. Baranov, I. V. Il'in, E. N. Mokhov, et al., JETP Lett. **82**, 441 (2005).
- ⁸ W. F. Koehl, B. B. Buckley, F. J. Heremans, et al., Nature **479**, 84 (2011).
- ⁹ P. G. Baranov, A. P. Bundakova, I. V. Borovykh, et al.,

JETP Lett. **86**, 202 (2007)

- ¹⁰ P. G. Baranov, A. P. Bundakova, A. A. Soltamova, et al., Phys. Rev. B **83**, 125203-1-12 (2011).
- ¹¹ P. G. Baranov, B. Ya. Ber, I. V. Ilyin, et al., J. Appl. Phys., **102**, 063713 (2007).
- ¹² V. S. Vainer, V. A. Il'in, Sov. Phys. Solid State **23**, 2126 (1981).
- ¹³ I. V. Borovykh, I. I. Proskuryakov, I. B. Klenina, et al., J. Phys. Chem. B **104**, 4222 (2000).
- ¹⁴ T. Wimbauer, B. K. Meyer, A. Hofstaetter, et al., Phys. Rev. B **56**, 7384 (1997).
- ¹⁵ N. Mizuochi, S. Yamasaki, H. Takizawa, et al., Phys. Rev. B **66**, 235202 (2002).
- ¹⁶ H. J. von Bardeleben, J. L. Cantin, I. Vickridge, G. Battistig Phys. Rev. B **62**, 10126 (2000).
- ¹⁷ N. B. Manson, J. P. Harrison, M. J. Sellars, Phys. Rev. B **74**, 104303 (2006).
- ¹⁸ G. G. Fedoruk, J. Appl. Spectr. **69**, 161 (2002).